



Chemical characteristics of submicron aerosols observed at the King Sejong Station in the northern Antarctic Peninsula from fall to spring

Saehee Lim^a, Meehye Lee^{a,*}, Tae Siek Rhee^b

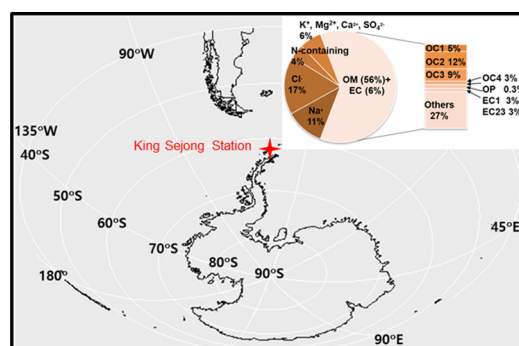
^a Dept. of Earth and Environmental Sciences, Korea University, Seoul, South Korea

^b Korea Polar Research Institute, Incheon, South Korea

HIGHLIGHTS

- OM and sea-salts comprised 85% of the PM₁ ($686 \pm 226 \text{ ng m}^{-3}$) at the KSG.
- The OC/EC ratio was greater than 10 with biogenic source for OC from the ocean.
- Char-EC was enhanced in biomass burning-impacted air from nearby continent.
- Soot-EC is a good tracer indicating local influence in Antarctic environment.

GRAPHICAL ABSTRACT



ARTICLE INFO

Article history:

Received 28 October 2018

Received in revised form 4 February 2019

Accepted 7 February 2019

Available online 22 February 2019

Editor: Jianmin Chen

Keywords:

PM₁
Elemental carbon
Organic carbon
Sea-salt
King Sejong Antarctic Station

ABSTRACT

The water-soluble ions and carbonaceous compounds of PM₁ were measured at the King Sejong Station (KSG) in the northern part of Antarctic Peninsula from March to November in 2009. As the sum of all measured species including organic matter [OM; organic carbon (OC)⁺1.9], the PM₁ mass reached a maximum of 936 ng m^{-3} with the mean of $686 \pm 226 \text{ ng m}^{-3}$. The most abundant constituents were OM ($389 \pm 109 \text{ ng m}^{-3}$) and sea-salts (Na^+ and Cl^- , $193 \pm 122 \text{ ng m}^{-3}$), which comprised 85% of the PM₁ mass. In contrast, the contribution of SO_4^{2-} was below 1% and its depletion relative to Na^+ was prevalent particularly during winter, which was attributed to the frost flowers on newly formed sea-ice surface. The OC concentration was the highest in fall and its subcomponents OC2 and OC3 were moderately correlated with sea-salts ($r = 0.5$), indicating the marine biogenic source for OC. The elemental carbon (EC) concentration was much lower than OC, leading to the mean OC/EC ratio over 10. While the charred fraction of EC (EC1) was elevated by the long-range transport of biomass burning plume from nearby continent, the mass fraction of soot-EC (EC23) was increased concurrently with enhanced NO_3^- , suggesting EC23 as a good indicator for local influence in pristine environments like Antarctic region.

© 2019 Published by Elsevier B.V.

1. Introduction

Aerosol plays a significant role in Earth's climate by affecting the global radiative balance (Boucher et al., 2013). Natural or anthropogenic aerosols are emitted to the atmosphere from various sources at the

* Corresponding author.

E-mail address: meehye@korea.ac.kr (M. Lee).

Earth surface or formed from gaseous precursors. Sea salts are important components of natural aerosols, particularly in the marine boundary layer. Sea-salt-containing aerosols are mechanically produced either over ice-free ocean surface by bubble bursting or over freshly formed sea ice (Monahan et al., 1986; Rankin et al., 2000; Wolff et al., 2003). Carbonaceous aerosol (CA) is of major interest owing to its atmospheric abundance, variety of emission sources, and significant climate effects. CA is often divided into organic carbon (OC) and elemental carbon (EC). OC is produced directly from biogenic emissions and combustion processes, and indirectly via formation of secondary particles from the oxidation of precursor gases. It is commonly considered to be the non-absorptive fraction of CA (Jacobson et al., 2000), whereas some OC fractions absorb solar radiation at short wavelength (Andreae and Gelencsér, 2006). EC, referred to as black carbon (BC) or soot, is primarily emitted by biomass burning and fossil-fuel combustion. It is a strong light-absorber and transported over long distance due to its small size in sub-micrometer (Bond et al., 2013; Ramanathan and Carmichael, 2008). For instance, in high-latitude or high-altitude areas EC transported from mid-latitudes (Bisiaux et al., 2012; Lim et al., 2017; Weller et al., 2013) has been identified as a significant contributor to accelerating snowmelt (Hansen and Nazarenko, 2004; Xu et al., 2016).

The Antarctic atmosphere consists of lower number and mass of aerosols as it is geographically isolated from human activities. Consequently, it provides unique place to study the atmospheric chemistry of pristine environment and thus to improve the understanding of the processes governing aerosol formation and transport (Jourdain and Legrand, 2002; Savoie et al., 1993; Weller and Wagenbach, 2007). However, its remote location and harsh environment hinders comprehensive study. Previous studies on aerosol composition reveal that sea-salts are most abundant (Minikin et al., 1998; Savoie et al., 1993; Teinilä et al., 2014; Wagenbach et al., 1998) and anthropogenic aerosols such as BC are often long-range transported from other continents (Chaubey et al., 2010; Weller et al., 2013; Wolff and Cachier, 1998).

Aerosols transported to Antarctic regions, particularly CA, show multiple source signature of the Southern Hemisphere, depending on the source strength and wind patterns. The King Sejong Station (KSG), located on the Barton Peninsula of King George Island, Antarctica, was a platform to study aerosol characteristics including chemical composition (Mishra et al., 2004), size distributions (Kim et al., 2017), and single particle properties (Eom et al., 2016). These studies focused mainly on

coarse-mode or nano-particles. Here, we report for the first time the chemical characteristics and the variation of sub-micron aerosols (PM_{10}) collected at KSG from fall to spring with emphasis on sea-salts and CA.

2. Methods

Sub-micron aerosols (PM_{10}) were collected at KSG, the Korean Antarctic Station in the northern part of the Antarctic Peninsula ($62^{\circ}13'S$, $58^{\circ}47'W$; Fig. 1), from March to November in 2009. A low-volume aerosol sampler with PM_{10} cyclone (URG, USA) was installed in the laboratory that was approximately 300 m southwest to the power generation building. We used the same inlet system as Mishra et al. (2004) described, which was specially designed for aerosol sampling at harsh environments. PM_{10} was collected at $16.7 L min^{-1}$ on 37-mm Teflon and Quartz fiber filters (Pall corp., USA) for analysis of water-soluble ions and carbonaceous compounds, respectively. Quartz fiber filters were pre-baked at $485^{\circ}C$ for 6 h. Total 16 samples were collected continuously at ~15-day interval. After collection, the filters were immediately stored in a freezer at lower than $-20^{\circ}C$. All filters were shipped in a refrigerated container from KSG to Korea Polar Research Institute in Korea.

Water-soluble ions laden on the Teflon filter were analyzed with an ion chromatography, and OC and EC were determined, according to the Interagency Monitoring of Protected Visual Environments thermal/optical reflectance protocol (i.e., IMP_TOR; Chow et al., 1993). The IMP_TOR method assumes that EC is a low-volatility carbon fraction that is not liberated in an oxygen-free environment till $550^{\circ}C$, allowing it to be separated from the more volatile OC that evolves at lower temperatures. Briefly, OC is measured as OC1, OC2, OC3, and OC4 liberated at different temperatures below $120^{\circ}C$, $250^{\circ}C$, $450^{\circ}C$, and $550^{\circ}C$, respectively. Some OC that is charred during the gradual increase in temperature is defined as pyrolyzed organic carbon (OP) after the split between OC and EC. EC1 and EC23 (sum of EC2 and EC3) are evolved under O_2 atmosphere at $550^{\circ}C$ and $700-800^{\circ}C$, respectively. Finally, OC and EC are reported as the sum of OC1, OC2, OC3, OC4, and OP and the sum of EC1 and EC23, respectively. The mass concentrations of all water-soluble ionic species and carbonaceous compounds were corrected for the mean blank values. The analytical lower detection limit (LDL) of water-soluble ions and total carbon (TC) was defined as 1 standard deviation

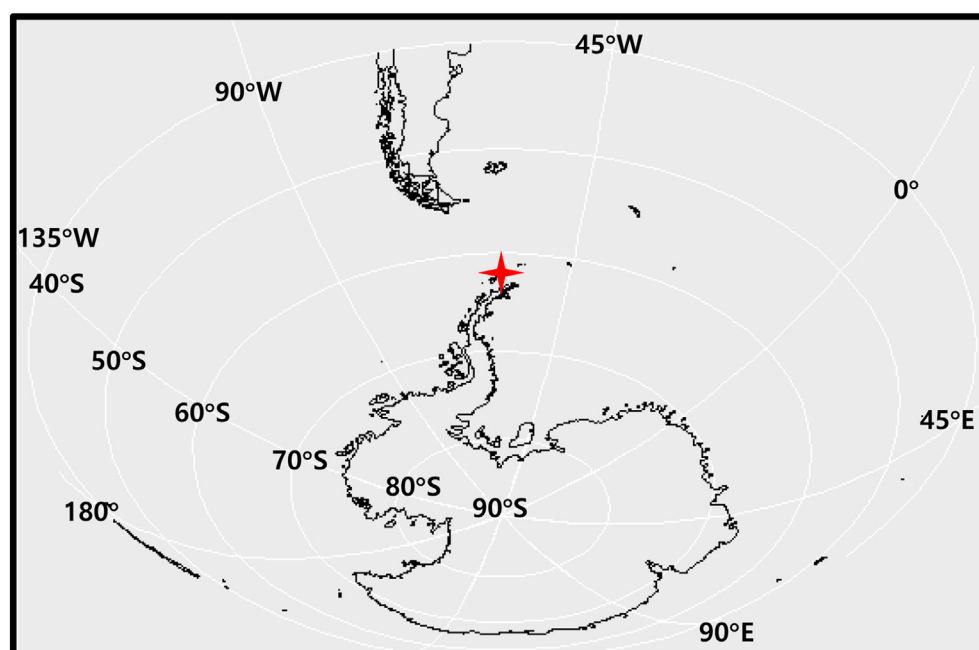


Fig. 1. Location of the King Sejong Station (KSG; $62^{\circ}13'S$, $58^{\circ}47'W$). The red symbol indicates KSG.

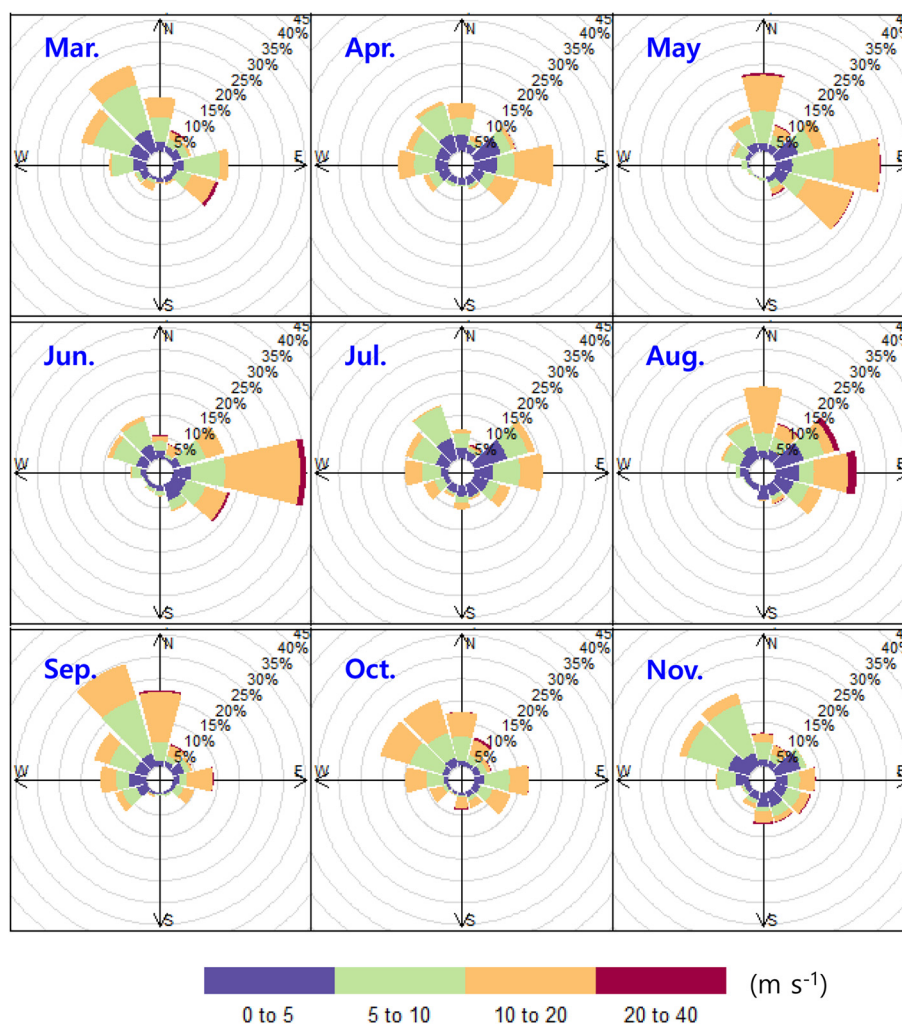


Fig. 2. Monthly wind rose measured at KSG from March to November in 2009. Sizes of the bins are proportional to the frequency of measurements. (For interpretation of the references to colour in this figure legend, the reader is referred to the web version of this article.)

(σ) of their blank concentrations. For statistics, the values below LDLs were replaced with $1/3\sigma$ of blank concentrations. Of the 16 samples, three samples were discarded due to analytical issues.

3. Results and discussion

3.1. Measurement summary

According to the local wind speed and direction measured at KSG (Fig. 2), easterly dominated in May and June (austral fall and early winter) and northwesterly in March, September, October, and November (austral early fall and spring). The other periods show shifting flow patterns. The synoptic wind field at 850 hPa (<https://www.esrl.noaa.gov/psd/data/gridded/data.ncep.reanalysis2.html>) also exhibits strong westerly winds passing over the southern part of South America in March, September and October (Fig. S1), indicating that the measured

wind pattern is in accordance with synoptic scale of meteorology as well.

The measurement results are summarized in Table 1, Fig. 3, and Fig. 4. In Antarctic coastal regions, aerosol mass is well represented by the sum of ionic species and carbonaceous compounds (Facchini et al., 2008; Kerminen et al., 2000; Teinilä et al., 2000), which were measured in this study. Adopting the upper-bound organic matter (OM)/OC ratio of 1.9 for mid-latitude rural areas (Bae et al., 2006; Simon et al., 2011), the sum of water-soluble ions, OM, and EC was assumed as PM_{10} mass. The PM_{10} mass ranged from 100 to 936 $ng\ m^{-3}$ with a mean of 686 $ng\ m^{-3}$. Of PM_{10} constituents, OC was predominant with a mean of $205 \pm 57\ ng\ m^{-3}$. The second most abundant species was Cl^{-} with a mean of $117 \pm 78\ ng\ m^{-3}$. As a result, OM and sea-salts (Na^{+} and Cl^{-}) occupied 85% of PM_{10} . The mean equivalent molar ratio of anion to cation was 0.52 ± 0.23 , indicating a greater contribution of alkalinity probably due to anion depletion, which will be discussed in Section 3.3.

Table 1

Statistical summary of the PM_{10} constituents measured at the King Sejong Station (KSG) from March to November in 2009.

Unit in $ng\ m^{-3}$	Water-soluble ions								Carbonaceous compounds		PM_{10}^a
	Na^{+}	Cl^{-}	NO_3^{-}	SO_4^{2-}	NH_4^{+}	Ca^{2+}	K^{+}	Mg^{2+}	OC	EC	
Mean	76.7	116.6	10.5	2.9	13.9	18.1	6.5	15.9	204.8	35.4	686.0
S.D. ^b	(46.7)	(78.2)	(9.5)	(1.4)	(4.4)	(8.5)	(4.9)	(8.9)	(57.2)	(18.8)	(226.5)

^a Sum of water-soluble ions, OM (OCx1.9), and EC.

^b One standard deviation.

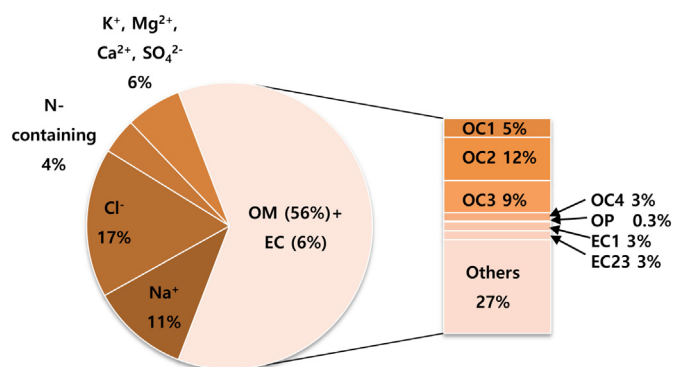


Fig. 3. The average chemical composition of PM₁ at KSG. PM₁ mass was estimated as the sum of the water-soluble ions, OM (OCx1.9), and EC mass concentrations.

3.2. Water-soluble ions

The water-soluble ions of PM₁ mass were an order of magnitude lower than that of annual total suspended particle (TSP) measured at KSG (year 2000–2001) (Mishra et al., 2004). Asmi et al. (2010) reported the ratio of coarse (PM_{8.5}) to fine (PM₁) sea-salts (sum of Na⁺ and Cl⁻) of 4 at the Aboa station in Antarctica that is located ~130 km far from the coast. These studies demonstrate that sea-salts are enriched in coarse mode particles of the Antarctic atmosphere. In the PM₁ of this study, OM was the most abundant with considerable contribution of sea-salts.

The mean ratio of Cl⁻ to Na⁺ was 1.75 ± 0.85 , which is close to the ratio in seawater (1.79). The mean ratio of Ca²⁺ to Na⁺ was 0.183, which is five times greater than that of seawater (0.038) but much smaller than those of soil and crust (1.78) (Bowen, 1979; Röhrlisberger et al., 2002). These results suggest that the influence of soil is not significant. Thus, the contribution of sea-salt to PM₁ was estimated using the equation of $\text{Cl}^- + 1.47 \times \text{Na}^+$, where 1.47 is the seawater ratio of $(\text{Na}^+ + \text{K}^+ + \text{Mg}^{2+} + \text{Ca}^{2+} + \text{SO}_4^{2-} + \text{HCO}_3^-) / \text{Na}^+$ (Asmi et al., 2010; Quinn and Bates, 2005). The sea-salts concentration was $248 \pm 133 \text{ ng m}^{-3}$, accounting for 88% of all water-soluble ions measured in this study and 36% of the PM₁ mass. In PM₁, the contribution of sea-salts was considerably large, whereas nitrogen-containing ionic species, i.e., nitrate and ammonium, together with EC comprised only 10%. It is primarily due to stormy current reinforced by westerly jet through the year.

The ionic concentrations were slightly higher in spring (October and November) and fall (April and May) by 61% and 34%, respectively, and lowered in winter (June–August) by 10% with respect to their mean values (Fig. 5). Both Na⁺ and Cl⁻ were also enhanced in spring and fall by ~80% and ~40%, respectively. This seasonal tendency of ionic species was consistent to what was previously observed for TSP at KSG (Mishra et al., 2004). The aerosol number concentrations also showed the maxima during the spring and summer and the minima during the winter (Kim et al., 2017).

The main factor controlling the seasonal loading of sea-salts is the variation in the distance from seawater. In winter, the seawater is frozen along the coast, resulting in the lesser release of sea-salts into the overlying air. It was seen in a firn core record retrieved in the James Ross island, which is about 230 km away from KSG (Aristarain and Delmas, 2002). In addition to the sea-salt transport over the shorter distance from the seawater during the spring and fall, wind direction and strength enhanced sea-salt loading at KSG (Kreutz et al., 2000; Kaspari et al., 2005). The sea-salt concentration was coincidentally high with wind speed in May, September, and October (Figs. 2 and 4). The southeasterly (from the Atlantic Ocean) and the northwesterly (from the Pacific Ocean) strong winds probably facilitated the transport of sea-salts into inland. The concentrations of Ca²⁺, K⁺ and SO₄²⁻ were relatively high during June and July with dominant easterly (>30%) (Fig. 2). It is

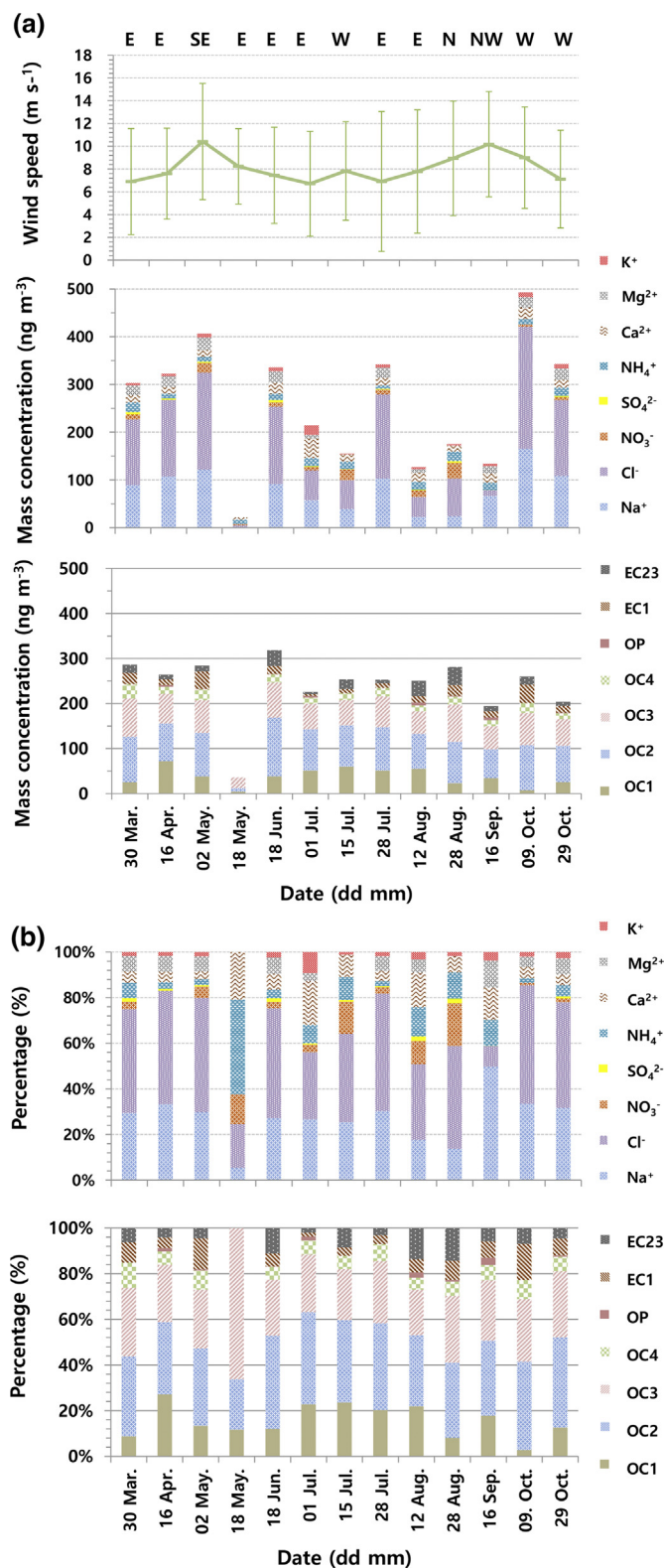


Fig. 4. (a) Mean wind speed with the mode of wind direction for each sampling period and mass concentrations of water-soluble ions, OC, and EC in PM₁, and (b) their fractions against PM₁ mass for the whole sampling period. Error bars for wind speed indicate ± 1 standard deviation. The dates on the horizontal axis are the starting day for each sample.

probably due to the impact of ornithogenic soil enriched with guano (Jourdain and Legrand, 2002; Ugolini, 1972), which is related to the topographical feature of KSG.

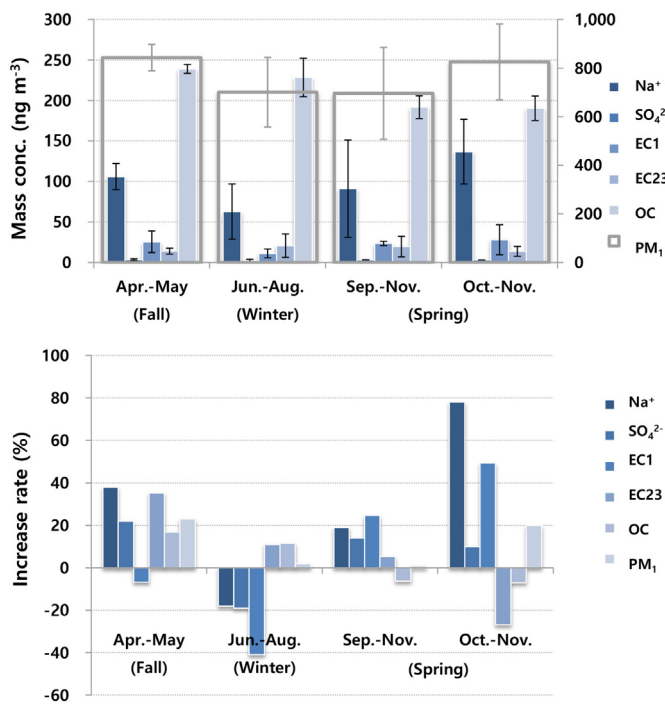


Fig. 5. For Na^+ , SO_4^{2-} , EC1, EC23, OC, and PM_{10} mass, the mean concentrations (top) and deviation from the mean (bottom) are compared for different periods. Apr.-May, Jun.-Aug., and Sep.-Nov. are defined as austral fall, winter, and spring, respectively. The data for Oct.-Nov. are further shown. In top panel, PM_{10} mass concentration is on the right y-axis and error bars denote ± 1 standard deviation.

3.3. SO_4^{2-} depletion relative to Na^+

In Antarctica, SO_4^{2-} aerosol mainly originates from sea-salts. In summer, biogenic SO_4^{2-} is added to bulk aerosols (Curran and Jones, 2000; Saltzman et al., 1986), enhancing SO_4^{2-} concentration in the atmosphere (Minikin et al., 1998; Wagenbach et al., 1998). For instance, the summer to winter ratio of SO_4^{2-} was up to 10 in size-segregated measurements at Dumont d'Urville, a coastal site (Jourdain and Legrand, 2002). The mean SO_4^{2-} concentration was $2.9 \pm 1.4 \text{ ng m}^{-3}$ in the present study, accounting for 0.4% of the PM_{10} mass. The SO_4^{2-} concentration was two orders of magnitude lower than that of TSP at the same site (Mishra et al., 2004). Our lower concentration was attributed to its smaller particle size and the lack of summer samples.

The nss-SO_4^{2-} mass estimated using the ratio of SO_4^{2-} to Na^+ in seawater (0.25) was less than zero, which resulted from the low SO_4^{2-} to Na^+ ratio (0.05 ± 0.04) (Fig. 6) and indicates a systematic depletion

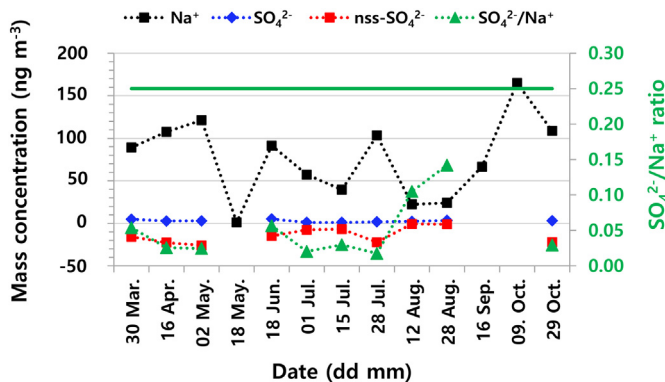


Fig. 6. The concentrations of Na^+ , SO_4^{2-} , and nss-SO_4^{2-} and the $\text{SO}_4^{2-}/\text{Na}^+$ ratio. The green line indicates the $\text{SO}_4^{2-}/\text{Na}^+$ ratio of sea water (0.25). (For interpretation of the references to colour in this figure legend, the reader is referred to the web version of this article.)

of SO_4^{2-} relative to Na^+ in sea-salt aerosols (Rankin et al., 2002, 2000). It is likely associated with the formation of frost flowers over the newly formed sea-ice surfaces, which are widespread around the Antarctica in the winter months (Minikin et al., 1998; Teinilä et al., 2014; Wagenbach et al., 1998). Frost flowers preferentially precipitate Na^+ and SO_4^{2-} as mirabilite ($\text{Na}_2\text{SO}_4 \cdot 10\text{H}_2\text{O}$) at below $-8.2 \text{ }^\circ\text{C}$. This fractionation was reported to remove most of SO_4^{2-} from seawater at the temperature commonly observed in the Antarctic winter (Rankin et al., 2002), and suggested as a significant source of sea-salt aerosol in winter (Wagenbach et al., 1998). Indeed, the SO_4^{2-} to Na^+ ratio was below 0.02 with the half of the mean SO_4^{2-} concentration during July-mid August (Fig. 6), revealing the significant SO_4^{2-} depletion during the winter.

3.4. OC and EC

OC was the most abundant component in PM_{10} and EC remained in low level (Fig. 3), resulting in the high OC/EC ratio over 10. The OC/EC ratio is typically below 5 at mid-latitudes. Among the OC sub-components, OC2 and OC3 concentrations were the highest and the refractory components of OC4 and OP concentrations were low. EC1 and EC23 were equally distributed in EC.

OC concentration was slightly elevated in fall by 17% and lowered in spring by 6% relative to the mean (Fig. 5). EC concentration increased in spring by 15% with elevated EC/TC ratio by 33%, and decreased in winter by 16% (Fig. 5). The temporal variation of EC concentration was similar to that of equivalent BC (EBC) that was observed for the same period (Kim et al., 2017), although the mean EC concentration was 2 times lower in our study. The discrepancy is probably due to different measurement techniques used in two studies (Petzold et al., 2013).

Since the water-soluble ionic species originated primarily from marine sources, the relationship between carbonaceous compounds and water-soluble ions were examined (Table S1). OC was moderately correlated with sea-salts including Na^+ and Cl^- ($R = 0.5$), suggesting that the considerable OC fraction was derived from the marine sources (Antony et al., 2011; Legrand et al., 2013). The temporal variation of OC concentration was unambiguous, being the highest in fall, right after the most extensive period of phytoplankton bloom in the southwest Atlantic sector of the Southern Ocean (Park et al., 2010), and lowest in spring (Fig. 5). Thus, it is highly likely that the enhanced OC was associated with marine biogenic activity particularly during the period of phytoplankton bloom. Both Na^+ and Cl^- were positively correlated with major OC fractions, OC2 and OC3 but negatively with minor fractions, OC1 and OP. This result suggests that among OC components, OC2 and OC3 were derived largely from marine sources. EC1 was also well correlated with Na^+ and Cl^- ($R = 0.6$) but for different reasons. EC can be subdivided into two classes and operationally defined based on the analytical method used: EC1 as char-EC and EC23 as soot-EC (Han et al., 2007, 2010). EC1 is known as a charred fraction of EC that can be emitted largely from incomplete combustion such as biomass burning (Han et al., 2010; Kumar and Attri, 2016; Lim et al., 2012). Therefore, EC1 and sea-salt concentrations were increased by strong wind that facilitated sea-salt production and EC1 transport. In contrast to EC1, EC23 is generally defined as a carbon particle forming at high temperature via gas-phase processes (Masiello, 2004) and its main source has been apportioned to be vehicle exhaust at mid-latitudes (Cao et al., 2005; Kim, 2004; Lim et al., 2012). In this study, EC23 was correlated with NO_3^- , SO_4^{2-} , and NH_4^+ ($R = 0.5, 0.4, \text{ and } 0.4$, respectively), implying fossil fuel combustion as its main source.

3.5. Enhanced OC and EC mass concentrations

The variation of OC and EC and its controlling factors were further investigated case-by-case. Based on their concentrations and fractional contribution to PM_{10} mass, three cases were selected and discussed as follows.

3.5.1. Enhanced OC with sea-salt during April 16–May 02, 2009

OC1 level increased by ~30% in fall and winter (Fig. 4b). The maximum OC1 concentration (72 ng m^{-3}) was found together with a moderately high OC concentration (241 ng m^{-3}) in the second half of April (Figs. 4a and 7). The enhancement of OC1 concentration was coincident with the high Na^+ concentration, which was increased by 50%. In addition, the moderate SO_4^{2-} depletion together with a slight Cl^- depletion was found, which suggests the influence of frost flowers. OC1 is semi-volatile carbon fraction by the analytical definition and thus probably associated with relatively fresh emission sources (Kim, 2004; Lim et al., 2012). These chemical features indicate that OC1 was associated with relatively fresh marine sources during the cold months, when its transport to the inland was promoted. It was partly supported by the dominant local winds of easterly (Fig. 4a) from the Weddell Sea with the largest area covered by sea ice annually (Cavaliere and Parkinson, 2008).

3.5.2. Long-range transport of biomass burning-driven EC during October 09–October 29, 2009

During this period, the maximum ionic mass concentration (493 ng m^{-3}) including Na^+ (165 ng m^{-3}) and Cl^- (256 ng m^{-3}) were observed with the maximum EC1 (41 ng m^{-3}) concentration and EC1/TC ratio (0.2) (Fig. 4a and Fig. 7). In contrast, the OC concentration was similar to its mean with the lowest OC1 concentration. A good correlation between EC1 and Na^+ was observed with the strong westerly during the entire sampling period. This period was distinguished by strong northwesterly with wind speed 30% higher than the mean (Fig. 2). Large-scale atmospheric circulation seemed to cause the efficient EC1 transport from other continents to the northern part of Antarctica. The broad EC peak of this case was in good agreement with the BC measurements at Neumayer in the Weddell Sea sector, where the maximum BC concentrations were observed in October and November (Weller et al., 2013). In South America as the main BC source region for the Weddell Sea region (Pereira et al., 2006), biomass burning typically peaks in September–October (van der Werf et al., 2006). The variability in biomass-burning source strength and large-scale meridional transport from low- and mid-latitudes were thus the primary factors controlling the annual variability of EC1 over the northern part of Antarctica.

3.5.3. Local effects during July 15–September 16, 2009

In the two cold months, the carbonaceous concentrations remained relatively low with the minimum level of ionic species. While Na^+ concentration was only the half of its mean, the maximum EC23 concentration was observed in August, albeit low (Fig. 7). It is also noteworthy that the relative fraction of EC23 and NO_3^- against mass increased, particularly in association with northerly or northeasterly winds below the annual mean ($8.3 \pm 1.2 \text{ m s}^{-1}$) under the relatively calm condition

(Fig. S2). The enhanced fraction of EC23 is likely due to the local influence of fossil-fuel combustion at KSG and therefore, EC23 is suggested as a good tracer for local effect at pristine environment such as the Antarctic region. The formation of NO_3^- could also be promoted by NO_x emissions in the station itself.

4. Conclusions

From March to November 2009, PM_{10} atmospheric particulate matter was collected to measure water-soluble ions and carbonaceous compounds at the King Sejong Station (KSG) in the northern part of Antarctic Peninsula. OC was the most abundant in PM_{10} and its concentration ranges from 36 to 265 ng m^{-3} with the mean of $205 \pm 57 \text{ ng m}^{-3}$. The next most abundant species were Cl^- ($117 \pm 78 \text{ ng m}^{-3}$) and Na^+ ($77 \pm 47 \text{ ng m}^{-3}$), confirming that sea-salts comprised a major fraction of PM_{10} in Antarctic region. When OC is converted to OM by multiplying the factor of 1.9, the mass of PM_{10} was in the range of 100 to 936 ng m^{-3} as the sum of all measured species. The average OM concentration was $389 \pm 109 \text{ ng m}^{-3}$ and accounted for 57% of PM_{10} mass. The sea-salt loading was enhanced by the strong northwesterly or easterly winds and the highest during the spring and fall. Particularly, SO_4^{2-} was depleted relative to Na^+ , which was associated with frost flowers over the newly formed sea-ice surfaces. The moderate correlation of OC with sea-salts and its seasonality suggest the predominant marine biogenic source for OC. The EC concentration was much lower than OC, leading to the high OC/EC ratio over 10. As the charred fraction of EC, EC1 was enhanced with strong northwesterly wind, which was attributed to the long-range transport of biomass-burning plume from nearby continent. The mass fraction of EC23 increased with NO_3^- under the calm condition during cold months, thus suggesting the EC23 as a good tracer for local effect in pristine Antarctic environment.

Acknowledgements

This research was supported by Basic Science Research Program through the National Research Foundation of Korea (NRF) funded by the Ministry of Science, Information, and Communications Technology & Future Planning (2017R1A2B4012143). S. Lim thanks the support by the Basic Science Research Program of NRF and the Ministry of Education (2015R1A6A3A01061393 and 2016R1D1A1B03934532). T. S. Rhee appreciates financial support from Korea Polar Research Programs (PM19050, PE19150, and PM14070).

Appendix A. Supplementary information

Supplementary information to this article can be found online at <https://doi.org/10.1016/j.scitotenv.2019.02.099>.

References

- Andreae, M.O., Gelencsér, A., 2006. Black carbon or brown carbon? The nature of light-absorbing carbonaceous aerosols. *Atmos. Chem. Phys.* 6, 3131–3148. <https://doi.org/10.5194/acp-6-3131-2006>.
- Antony, R., Mahalinganathan, K., Thamban, M., Nair, S., 2011. Organic carbon in Antarctic snow: spatial trends and possible sources. *Environ. Sci. Technol.* 45, 9944–9950. <https://doi.org/10.1021/es203512t>.
- Aristarain, A.J., Delmas, R.J., 2002. Snow chemistry measurements on James Ross Island (Antarctic Peninsula) showing sea-salt aerosol modifications. *Atmos. Environ.* 36, 765–772. [https://doi.org/10.1016/S1352-2310\(01\)00362-4](https://doi.org/10.1016/S1352-2310(01)00362-4).
- Asmi, E., Frey, A., Virkkula, A., Ehn, M., Manninen, H.E., Timonen, H., Tolonen-Kivimäki, O., Aurela, M., Hillamo, R., Kulmala, M., 2010. Hygroscopicity and chemical composition of Antarctic sub-micrometre aerosol particles and observations of new particle formation. *Atmos. Chem. Phys.* 10, 4253–4271. <https://doi.org/10.5194/acp-10-4253-2010>.
- Bae, M.-S., Schauer, J.J., Turner, J.R., 2006. Estimation of the monthly average ratios of organic mass to organic carbon for fine particulate matter at an urban site. *Aerosol Sci. Technol.* 40, 1123–1139. <https://doi.org/10.1080/02786820601004085>.
- Bisiaux, M.M., Edwards, R., McConnell, J.R., Albert, M.R., Anschutz, H., Neumann, T.A., Isaksson, E., Penner, J.E., 2012. Variability of black carbon deposition to the East Antarctic Plateau, 1800–2000 AD. *Atmos. Chem. Phys.* 12, 3799–3808. <https://doi.org/10.5194/acp-12-3799-2012>.

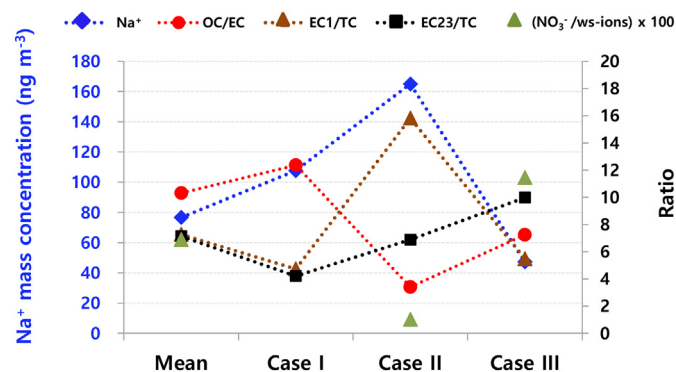


Fig. 7. Comparison of chemical characteristics of PM_{10} for the selected cases: Case I for April 16, 2009–May 02, 2009, Case II for October 09, 2009–October 29, 2009, and Case III for July 15, 2009–September 16, 2009.

- Bond, T.C., Doherty, S.J., Fahey, D.W., Forster, P.M., Berntsen, T., DeAngelo, B.J., Flanner, M.G., Ghan, S., Kärcher, B., Koch, D., Kinne, S., Kondo, Y., Quinn, P.K., Sarofim, M.C., Schultz, M.G., Schulz, M., Venkataraman, C., Zhang, H., Zhang, S., Bellouin, N., Guttikunda, S.K., Hopke, P.K., Jacobson, M.Z., Kaiser, J.W., Klimont, Z., Lohmann, U., Schwarz, J.P., Shindell, D., Storelvmo, T., Warren, S.G., Zender, C.S., 2013. Bounding the role of black carbon in the climate system: a scientific assessment. *J. Geophys. Res. Atmos.* 118, 5380–5552. <https://doi.org/10.1002/jgrd.50171>.
- Boucher, O., Randall, D., Artaxo, P., Bretherton, C., Feingold, G., Forster, P., Kerminen, V.-M., Kondo, Y., Liao, H., Lohmann, U., Rasch, P., Satheesh, S.K., Sherwood, S., Stevens, B., Zhang, X.Y., 2013. *Clouds and aerosols. Climate Change 2013: The Physical Science Basis. Contribution of Working Group I to the Fifth Assessment Report of the Intergovernmental Panel on Climate Change.* Cambridge University Press, Cambridge, United Kingdom and New York, NY, USA.
- Bowen, H.J.M., 1979. *Environmental Chemistry of the Elements.* Academic Press, London.
- Cao, J.J., Wu, F., Chow, J.C., Lee, S.C., Li, Y., Chen, S.W., An, Z.S., Fung, K.K., Watson, J.G., Zhu, C.S., Liu, S.X., 2005. Characterization and source apportionment of atmospheric organic and elemental carbon during fall and winter of 2003 in Xi'an, China. *Atmos. Chem. Phys.* 5, 3127–3137. <https://doi.org/10.5194/acp-5-3127-2005>.
- Cavaliere, D.J., Parkinson, C.L., 2008. Antarctic Sea ice variability and trends, 1979–2006. *J. Geophys. Res.* 113, C07004. <https://doi.org/10.1029/2007JC004564>.
- Chaubey, J.P., Moorthy, K.K., Babu, S.S., Nair, V.S., Tiwari, A., 2010. Black carbon aerosols over coastal Antarctica and its scavenging by snow during the southern hemispheric summer. *J. Geophys. Res.* 115, D10210. <https://doi.org/10.1029/2009JD013381>.
- Chow, J.C., Watson, J.G., Pritchett, L.C., Pierson, W.R., Frazier, C.A., Purcell, R.G., 1993. The dri thermal/optical reflectance carbon analysis system: description, evaluation and applications in U.S. air quality studies. *Atmos. Environ. Part A. Gen. Top.* 27, 1185–1201. [https://doi.org/10.1016/0960-1686\(93\)90245-T](https://doi.org/10.1016/0960-1686(93)90245-T).
- Curran, M.A.J., Jones, G.B., 2000. Dimethyl sulfide in the Southern Ocean: seasonality and flux. *J. Geophys. Res. Atmos.* 105, 20451–20459. <https://doi.org/10.1029/2000JD900176>.
- Eom, H.-J., Gupta, D., Cho, H.-R., Hwang, H.J., Do Hur, S., Gim, Y., Ro, C.-U., 2016. Single-particle investigation of summertime and wintertime Antarctic sea spray aerosols using low-particle EPMA, Raman microspectrometry, and ATR-FTIR imaging techniques. *Atmos. Chem. Phys.* 16, 13823–13836. <https://doi.org/10.5194/acp-16-13823-2016>.
- Facchini, M.C., Rinaldi, M., Decesari, S., Carbone, C., Finessi, E., Mircea, M., Fuzzi, S., Ceburnis, D., Flanagan, R., Nilsson, E.D., de Leeuw, G., Martino, M., Wolstjen, J., O'Dowd, C.D., 2008. Primary submicron marine aerosol dominated by insoluble organic colloids and aggregates. *Geophys. Res. Lett.* 35, L17814. <https://doi.org/10.1029/2008GL034210>.
- Han, Y., Cao, J., Chow, J.C., Watson, J.G., An, Z., Jin, Z., Fung, K., Liu, S., 2007. Evaluation of the thermal/optical reflectance method for discrimination between char- and soot-EC. *Chemosphere* 69, 569–574. <https://doi.org/10.1016/j.chemosphere.2007.03.024>.
- Han, Y.M., Cao, J.J., Lee, S.C., Ho, K.F., An, Z.S., 2010. Different characteristics of char and soot in the atmosphere and their ratio as an indicator for source identification in Xi'an, China. *Atmos. Chem. Phys.* 10, 595–607. <https://doi.org/10.5194/acp-10-595-2010>.
- Hansen, J., Nazarenko, L., 2004. Soot climate forcing via snow and ice albedos. *Proc. Natl. Acad. Sci. U. S. A.* 101, 423–428. <https://doi.org/10.1073/pnas.2237157100>.
- Jacobson, M.C., Hansson, H.-C., Noone, K.J., Charlson, R.J., 2000. Organic atmospheric aerosols: review and state of the science. *Rev. Geophys.* 38, 267–294. <https://doi.org/10.1029/1998RG000045>.
- Jourdain, B., Legrand, M., 2002. Year-round records of bulk and size-segregated aerosol composition and HCl and HNO₃ levels in the Dumont d'Urville (coastal Antarctica) atmosphere: implications for sea-salt aerosol fractionation in the winter and summer. *J. Geophys. Res.* 107, 4645. <https://doi.org/10.1029/2002JD002471>.
- Kaspari, S., Dixon, D.A., Sneed, S.B., Handley, M.J., 2005. Sources and transport pathways of marine aerosol species into West Antarctica. *Ann. Glaciol.* 41, 1–9. <https://doi.org/10.3189/172756405781813221>.
- Kerminen, V.-M., Teinilä, K., Hillamo, R., 2000. Chemistry of sea-salt particles in the summer Antarctic atmosphere. *Atmos. Environ.* 34, 2817–2825. [https://doi.org/10.1016/S1352-2310\(00\)00089-3](https://doi.org/10.1016/S1352-2310(00)00089-3).
- Kim, E., 2004. Improving source identification of fine particles in a rural northeastern U.S. area utilizing temperature-resolved carbon fractions. *J. Geophys. Res.* 109, D09204. <https://doi.org/10.1029/2003JD004199>.
- Kim, J., Jun Yoon, Y., Gim, Y., Jin Kang, H., Hee Choi, J., Park, K.T., Yong Lee, B., 2017. Seasonal variations in physical characteristics of aerosol particles at the King Sejong Station, Antarctic Peninsula. *Atmos. Chem. Phys.* 17, 12985–12999. <https://doi.org/10.5194/acp-17-12985-2017>.
- Kreutz, K.J., Mayewski, P.A., Pittalwala, I.I., Meeker, L.D., Twickler, M.S., Whitlow, S.I., 2000. Sea level pressure variability in the Amundsen Sea region inferred from a West Antarctic glaciochemical record. *J. Geophys. Res. Atmos.* 105, 4047–4059. <https://doi.org/10.1029/1999JD901069>.
- Kumar, A., Attri, A.K., 2016. Biomass combustion a dominant source of carbonaceous aerosols in the ambient environment of Western Himalayas. *Aerosol Air Qual. Res.* 16, 519–529. <https://doi.org/10.4209/aaqr.2015.05.0284>.
- Legrand, M., Preunkert, S., Jourdain, B., Guilhaumet, J., Fain, X., Alekhina, I., Petit, J.R., 2013. Water-soluble organic carbon in snow and ice deposited at alpine, Greenland, and Antarctic sites: a critical review of available data and their atmospheric relevance. *Clim. Past* 9, 2195–2211. <https://doi.org/10.5194/cp-9-2195-2013>.
- Lim, S., Lee, M., Lee, G., Kim, S., Yoon, S., Kang, K., 2012. Ionic and carbonaceous compositions of PM₁₀, PM_{2.5} and PM_{1.0} at Gosan ABC Superstation and their ratios as source signature. *Atmos. Chem. Phys.* 12, 2007–2024. <https://doi.org/10.5194/acp-12-2007-2012>.
- Lim, S., Fain, X., Ginot, P., Mikhaleiko, V., Kutuzov, S., Paris, J.-D., Kozachek, A., Laj, P., 2017. Black carbon variability since preindustrial times in the eastern part of Europe reconstructed from Mt. Elbrus, Caucasus, ice cores. *Atmos. Chem. Phys.* 17, 3489–3505. <https://doi.org/10.5194/acp-17-3489-2017>.
- Masiello, C.A., 2004. New directions in black carbon organic geochemistry. *Mar. Chem.* 92, 201–213. <https://doi.org/10.1016/j.marchem.2004.06.043>.
- Minikin, A., Legrand, M., Hall, J., Wagenbach, D., Kleefeld, C., Wolff, E., Pasteur, E.C., Ducroz, F., 1998. Sulfur-containing species (sulfate and methanesulfonate) in coastal Antarctic aerosol and precipitation. *J. Geophys. Res. Atmos.* 103, 10975–10990. <https://doi.org/10.1029/98JD00249>.
- Mishra, V.K., Kim, K.-H., Hong, S., Lee, K., 2004. Aerosol composition and its sources at the King Sejong Station, Antarctic peninsula. *Atmos. Environ.* 38, 4069–4084. <https://doi.org/10.1016/j.atmosenv.2004.03.052>.
- Monahan, E.C., Spiel, D.E., Davidson, K.L., 1986. A Model of Marine Aerosol Generation Via Whitecaps and Wave Disruption. Springer, Dordrecht, pp. 167–174. https://doi.org/10.1007/978-94-009-4668-2_16.
- Park, J., Oh, I.-S., Kim, H.-C., Yoo, S., 2010. Variability of SeaWiFS chlorophyll-a in the southwest Atlantic sector of the Southern Ocean: strong topographic effects and weak seasonality. *Deep Sea Res. Part I Oceanogr. Res. Pap.* 57, 604–620. <https://doi.org/10.1016/j.DSR.2010.01.004>.
- Pereira, E.B., Evangelista, H., Pereira, K.C.D., Cavalcanti, I.F.A., Setzer, A.W., 2006. Apportionment of black carbon in the South Shetland Islands, Antarctic Peninsula. *J. Geophys. Res.* 111, D03303. <https://doi.org/10.1029/2005JD006086>.
- Petzold, A., Ogren, J.A., Fiebig, M., Laj, P., Li, S.-M., Baltensperger, U., Holzner-Popp, T., Kinne, S., Pappalardo, G., Sugimoto, N., Wehrli, C., Wiedensohler, A., Zhang, X.-Y., 2013. Recommendations for reporting “black carbon” measurements. *Atmos. Chem. Phys.* 13, 8365–8379. <https://doi.org/10.5194/acp-13-8365-2013>.
- Quinn, P.K., Bates, T.S., 2005. Regional aerosol properties: comparisons of boundary layer measurements from ACE 1, ACE 2, Aerosols99, INDOEX, ACE Asia, TARFOX, and NEAQS. *J. Geophys. Res. Atmos.* 110, 202. <https://doi.org/10.1029/2004JD004755>.
- Ramanathan, V., Carmichael, G., 2008. Global and regional climate changes due to black carbon. *Nat. Geosci.* 1, 221–227. <https://doi.org/10.1038/ngeo156>.
- Rankin, A.M., Auld, V., Wolff, E.W., 2000. Frost flowers as a source of fractionated sea salt aerosol in the polar regions. *Geophys. Res. Lett.* 27, 3469–3472. <https://doi.org/10.1029/2000GL011771>.
- Rankin, A.M., Wolff, E.W., Martin, S., 2002. Frost flowers: implications for tropospheric chemistry and ice core interpretation. *J. Geophys. Res. Atmos.* 107, AAC 4–1–AAC 4–15. <https://doi.org/10.1029/2002JD002492>.
- Röthlisberger, R., Mulvaney, R., Wolff, E.W., Hutterli, M.A., Bigler, M., Sommer, S., Jouzel, J., 2002. Dust and sea salt variability in central East Antarctica (Dome C) over the last 45 kyr and its implications for southern high-latitude climate. *Geophys. Res. Lett.* 29, 24–1–24–4. <https://doi.org/10.1029/2002GL015186>.
- Saltzman, E.S., Savoie, D.L., Prospero, J.M., Zika, R.G., 1986. Methanesulfonic acid and non-sea-salt sulfate in Pacific air: regional and seasonal variations. *J. Atmos. Chem.* 4, 227–240. <https://doi.org/10.1007/BF00052002>.
- Savoie, D.L., Prospero, J.M., Larsen, R.J., Huang, F., Izaguirre, M.A., Huang, T., Snowdon, T.H., Custals, L., Sanderson, C.G., 1993. Nitrogen and sulfur species in Antarctic aerosols at Mawson, Palmer Station, and Marsh (King George Island). *J. Atmos. Chem.* 17, 95–122. <https://doi.org/10.1007/BF00702821>.
- Simon, H., Bhavs, P.V., Swall, J.L., Frank, N.H., Malm, W.C., 2011. Determining the spatial and seasonal variability in OM/OC ratios across the US using multiple regression. *Atmos. Chem. Phys.* 11, 2933–2949. <https://doi.org/10.5194/acp-11-2933-2011>.
- Teinilä, K., Kerminen, V.-M., Hillamo, R., 2000. A study of size-segregated aerosol chemistry in the Antarctic atmosphere. *J. Geophys. Res.* 105, 3893–3904. <https://doi.org/10.1029/1999JD901033>.
- Teinilä, K., Frey, A., Hillamo, R., Tülp, H.C., Weller, R., 2014. A study of the sea-salt chemistry using size-segregated aerosol measurements at coastal Antarctic station Neumayer. *Atmos. Environ.* 96, 11–19. <https://doi.org/10.1016/j.atmosenv.2014.07.025>.
- Ugolini, F.C., 1972. Ornithogenic soils of Antarctica. In: Liano, G.A. (Ed.), *Antarctic Terrestrial Biology.* American Geophysical Union, Washington, DC, pp. 181–193. <https://doi.org/10.1002/9781118664667.ch9>.
- van der Werf, G.R., Randerson, J.T., Giglio, L., Collatz, G.J., Kasibhatla, P.S., Arellano, A.F., 2006. Interannual variability in global biomass burning emissions from 1997 to 2004. *Atmos. Chem. Phys.* 6, 3423–3441. <https://doi.org/10.5194/acp-6-3423-2006>.
- Wagenbach, D., Ducroz, F., Mulvaney, R., Keck, L., Minikin, A., Legrand, M., Hall, J.S., Wolff, E.W., 1998. Sea-salt aerosol in coastal Antarctic regions. *J. Geophys. Res.* 103, 10961–10974. <https://doi.org/10.1029/97JD01804>.
- Weller, R., Wagenbach, D., 2007. Year-round chemical aerosol records in continental Antarctica obtained by automatic samplings. *Tellus Ser. B. Chem. Phys. Meteorol.* 59, 755–765. <https://doi.org/10.1111/j.1600-0889.2007.00293.x>.
- Weller, R., Minikin, A., Petzold, A., Wagenbach, D., König-Langlo, G., 2013. Characterization of long-term and seasonal variations of black carbon (BC) concentrations at Neumayer, Antarctica. *Atmos. Chem. Phys.* 13, 1579–1590. <https://doi.org/10.5194/acp-13-1579-2013>.
- Wolff, E.W., Cachier, H., 1998. Concentrations and seasonal cycle of black carbon in aerosol at a coastal Antarctic station. *J. Geophys. Res. Atmos.* 103, 11033–11041. <https://doi.org/10.1029/97JD01363>.
- Wolff, E.W., Rankin, A.M., Röthlisberger, R., 2003. An ice core indicator of Antarctic Sea ice production? *Geophys. Res. Lett.* 30, 2158–2161. <https://doi.org/10.1029/2003GL018454>.
- Xu, Y., Ramanathan, V., Washington, W.M., 2016. Observed high-altitude warming and snow cover retreat over Tibet and the Himalayas enhanced by black carbon aerosols. *Atmos. Chem. Phys.* 16, 1303–1315. <https://doi.org/10.5194/acp-16-1303-2016>.